Atmos. Chem. Phys. Discuss., 6, 2151–2174, 2006
www.atmos-chem-phys-discuss.net/6/2151/2006/

Atmospheric Chemistry and Physics Discussions

Technical note: Characterization of a static thermal-gradient CCN counter

G. P. Frank[1], **U. Dusek**[1], **and M. O. Andreae**[1]

[1]Biogeochemistry Department, Max Planck Institute for Chemistry, P.O. Box 3060, 55020 Mainz, Germany

Received: 22 November 2005 – Accepted: 31 January 2006 – Published: 29 March 2006

Correspondence to: G. P. Frank (gfrank@mpch-mainz.mpg.de)

Abstract

The static (parallel-plate thermal-gradient) diffusion chamber (SDC) was one of the first instruments designed to measure cloud condensation nuclei (CCN) concentrations as a function of supersaturation. It has probably also been the most widely used type of CCN counter. This paper describes the detailed experimental characterization of a SDC CCN counter, including calibration with respect to supersaturation and particle number concentration. In addition, we investigated the proposed effect of lowered supersaturation because of water vapor depletion with increasing particle concentration. The results obtained gives a larger understanding why and in which way it is necessary to calibrate the SDC CCN counter. The calibration method is described in detail as well. The method can, in parts, be used for calibrations also for other types of CCN counters.

We conclude the following: 1) it is important to experimentally calibrate SDC CCN counters with respect to supersaturation, and not only base the supersaturation on the theoretical description of the instrument; 2) the number concentration calibration needs to be performed as a function of supersaturation, also for SDC CCN counter using the photographic technique; and 3) we observed no evidence that water vapor depletion lowered the supersaturation.

1 Introduction

The static diffusion chamber (SDC) was among the first instruments designed to measure CCN concentration as a function of supersaturation (Wieland, 1956). The parallel-plate thermal-gradient SDC CCN counter works with a temperature difference between two horizontal wetted plates, the lower plate colder than the upper to avoid buoyancy. In equilibrium this gives rise to linear gradients of temperature and water vapor partial pressure between the two plates. Because of the non-linear dependence of the saturation vapor pressure on temperature, a parabolic supersaturation (S) profile is

ACPD

6, 2151–2174, 2006

established. The maximum S is reached close to the centre of the chamber, and by locating the sensing volume in the central part, all particles in that volume will be exposed to a supersaturation close to the maximum. This supersaturation is directly related to the temperature difference between the plates. However, it has proven to be difficult to determine the temperatures exactly at the surfaces of the plates. Evaporation of water vapor at the warm plate and condensation on the cold plate makes the temperatures at the surfaces different from the temperatures inside the plates, where the temperature sensors are positioned. Heat can also conduct through the walls of the chamber. These effects lead to a smaller temperature difference than expected.

Originally, the number of cloud droplets activated in the chamber most often was counted using a manual photographic technique (e.g., Twomey, 1959), but later, measurements of light scattering have been used (e.g., Lala and Jiusto, 1977; de Oliveira and Vali, 1995; Delene et al., 1998; Snider and Brenguier 2000). In newer CCN counters of this type, the photographic technique has again been used, now with video or CCD cameras, together with modern image processing methods (e.g. Giebl et al., 2002). This principle is also utilized in the CCN counter used in this study (Roberts et al., 2001) and in the previously commercially available instrument, Model M1, from DH Associates, which was used for example in Cruz and Pandis (1997), Jennings et al. (1998), and Corrigan and Novakov (1999). Converting the number of droplets in the sensing volume to CCN concentration requires precise knowledge of the volume. However, it has proven to be difficult to measure this volume precisely enough, and a calibration of CCN concentration vs. droplet number is therefore needed. This work has also showed that the calibrated sensing volume has an apparent dependence on the supersaturation.

Hudson (1993) and McMurry (2000) presented overviews of CCN instruments. The increased interest in investigating effects of aerosols on clouds and climate has, in addition, lead to several recent CCN counter developments, e.g. Ji et al. (1998), Holländer et al. (2002), Otto et al. (2002), VanReken et al. (2004), and Roberts and Nenes (2005).

Despite that SDC type CCN counters has been used for several decades, knowledge

about the non-ideal behavior and the importance of proper calibration seem still not to be widely spread. Traditionally has SDC CCN counters, as well as most other CCN counter types, been assumed to be absolute devices, i.e. the supersaturation can be determined by the temperature difference of the plates only, and the number concentration by knowing the measuring volume (Hudson, 1993). However, it has been made clear that this is often not the case.

When using the photographic technique, a series of pictures are taken during the cycle of droplet activation and growth, and the assumption is made that the picture with the highest count is the best estimator of the true CCN concentration (de Oliveira and Vali, 1995). When the light scattering technique was introduced, concentration calibration became necessary, since the scattered light per drop has a dependence on the supersaturation because the droplets grow larger at higher supersaturations (e.g. Lala and Juisto, 1977; de Oliveira and Vali, 1995). The calibration was first made by calibrating the scattered light signal against the manual photographic technique (Lala and Juisto, 1977; de Oliveira and Vali, 1995). Delene and Dechsler (2000) compared, in addition, the scattered signal to the concentration measured in parallel with a condensation particle counter (CPC), using monodisperse particles of a size large enough so that they all should activate in the CCN counter. This latter method has been more used since then, also in the work described in this paper, and, as will be shown, the earlier assumptions have clear limitations. Using the picture with the highest count introduces a dependence of the apparent sensing volume on the supersaturation.

Cruz and Pandis (1997) observed a discrepancy between the adjusted instrumental supersaturation and the theoretically calculated critical supersaturation for activation, when measuring monodisperse ammonium sulfate and sodium chloride particles. Giebl et al. (2002), Snider et al. (2003), and Bilde and Svenningsson (2004) confirmed this result.

Validations of the accuracy of CCN counter instruments have earlier often been made as intercomparisons, e.g. in CCN counter workshops (Hudson, 1993; McMurry, 2000; Holländer, 2002). Lately, has the need for more detailed calibrations been re-

ACPD
6, 2151–2174, 2006

alized. However, CCN measurements without fully calibrating the instruments are still performed, e.g. Jennings et al. (1998) and Roberts et al. (2003).

The objectives of this paper are to characterize and, in more detail, investigate features of the SDC type CCN counter, in order to better learn how to calibrate the instrument type. A calibration method is described as well. A final objective is to point out that calibration is of great importance for accurate CCN measurements.

2 Description of the Mainz CCN counter

The CCN counter characterized in this study was developed at the Max Planck Institute for Chemistry in Mainz, Germany, by G. Roberts and P. Guyon (Roberts et al., 2001; Roberts, 2001) (Fig. 1), and is similar to the one described by Lala and Juisto (1977). The diameter of the chamber is 80 mm and the distance between the plates (H) is 10 mm. Filter papers on the upper and lower plates are kept wetted continuously by distilled water through a water supply system. The temperature of the upper plate is allowed to float, and the temperature of the lower plate is controlled in order to reach the requested temperature difference. Sensitivity studies show that the temperatures at the plates must be controlled within ±0.1°C to keep the S within ±0.05% variation, and the fluctuations during measurements are usually lower than that. In contrast to the Lala and Juisto CCN counter, our instrument uses laser illumination (670 nm) and a video camera to detect the activated droplets in the CCN chamber, and image analysis software to count the number of droplets in the sensing volume. The laser beam is widened by a lens and illuminates a slit. The width of the sensing volume is determined by the slit width (which can be changed), and the length and height are set in the image analysis software.

A typical measurement cycle starts with setting the supersaturation by adjusting the temperature difference between the plates. After that, the chamber is flushed with a sample air flow in the range from 1 to 3 l/min for 10–20 s, and then closed. While the chamber is closed, the air is passing through the CCN counter in a by-pass line so as

not to interrupt the air flow in the sampling line. During the closed period of 12 to 15 s, the camera takes up to a few images per second (camera speed is adjustable). The image analysis software counts the number of droplets in each image, and the CCN concentration calculation is based on the image/images with the highest number of droplets. The time resolution is typically 50–60 s between successive measurements, with a change of S in-between.

3 Characterization

Because of the difficulties discussed above, it has proven necessary to calibrate the instrument with respect to both S and CCN number concentration. We have used a similar method to that presented in Cruz and Pandis (1997), Corrigan and Novakov (1999), Giebl et al. (2002), and Bilde and Svenningsson (2004).

3.1 Calibration set-up

The calibration set-up consists of an atomizer (both a compressed-air nebulizer and a TSI 3076 Constant Output Atomizer were used), a Differential Mobility Analyzer (DMA; TSI 3071 Electrostatic Classifier, somewhat modified and changed to closed-loop arrangement (Jokinen and Mäkelä, 1997)), and a Condensation Particle Counter (CPC; TSI 3762), see Fig. 2. Pure sodium chloride or ammonium sulfate particles are generated from a water solution by the atomizer, and thereafter dried. The DMA operates with an aerosol flow to sheath flow ratio of 1:10, and selects particles within a narrow size range. Multiply charged particles of larger size will also penetrate the DMA, but these do not interfere with the calibration, see below. The CCN counter measures the CCN concentration as a function of S, of particles of the selected size, and the CPC counts the total number of aerosol particles of the same size. The CPC can be connected in parallel or in series to the CCN counter, using an internal bypass. The same set-up is used for all three types of calibrations/characterizations. However, for

the supersaturation calibration and for the study of water vapor depletion, the CPC is not needed.

3.2 Supersaturation calibration

The CCN counter was calibrated with respect to supersaturation, by using salt particles of known size and composition. Since the critical supersaturation for activation of these particles can be accurately calculated with the Köhler equation (e.g., Pruppacher and Klett, 1997), we consider this method to be more reliable than calculating the supersaturation from the measured temperatures of the plates.

The DMA was set to select a narrow size range, and the activated particles were counted in the CCN counter as a function of the nominal S. For the calibration of the lowest S, the particle size was varied at constant nominal S. Figure 3a shows an example of a calibration scan using ammonium sulfate particles of 30 nm in diameter. The CCN concentration is plotted against nominal S, calculated from the measured temperature difference of the plates, using an approximation of Eq. (A4). The nominal supersaturation at which 50% of the particles are activated (S_{exp}) is found by fitting a function to the spectrum:

$$f(S) = a \cdot erf\left(\frac{S-b}{c}\right) \quad (1)$$

where *erf* is the cumulative normal distribution (the so-called error function) and a, b and c are coefficients that are varied to obtain the best fit. S_{exp} is determined numerically as the supersaturation where f reaches half its maximum value ($f(S_{exp})=a/2$). The activation curve is steep and it is thus possible to determine S_{exp} with high accuracy. The CCN that appear below 1.5% S originate from a small fraction of doubly charged particles with geometric diameter larger than 30 nm. The influence of doubly charged particles on S_{exp} could be neglected due to their low concentrations. From the upper and lower bounds of the fit, the uncertainty of S_{exp} (95% confidence interval) could be derived (e.g. ±0.03% in S (absolute) for the 30-nm particles).

ACPD
6, 2151–2174, 2006

S_{exp} was determined for ammonium sulfate and sodium chloride particles with dry diameters between 20 nm and 88 nm. S_{exp} was then compared to the actual critical supersaturations, (S_c), calculated with the Köhler equation for each particle size and composition (Fig. 3b). Non-idealities of the solution droplet were taken into account by letting the van't Hoff factor (i) vary with molality (M) according to the data of Low (1969), who presented data for $M>0.1$. For $M<0.1$, the regression suggested by Young and Warren (1991) was used for ammonium sulfate. For sodium chloride at $M<0.1$, no regression was available, and the last data point from Low at $M=0.1$, $i=1.87$, and the value of $i=2$ at $M=0$ were linearly interpolated. Sodium chloride particles are assumed to be of cubic shape, and a form factor of 1.08 was used to calculate the equivalent volume diameter, whereas the ammonium sulfate particles are assumed to be spherical (Mitra et al., 1992; Hinds, 1999). The use of the van't Hoff factor and the form factor increased the R^2 of the regression fit from 0.980 to 0.994.

The actual supersaturation in the CCN counter is roughly half of the nominal supersaturation (k=0.544±0.013 and d=0.016±0.022, where 0.013 and 0.022 are one standard deviation of the regression constants). This is a relatively large difference, but it is in agreement with the assumption that the temperature difference is lower than expected. The data obtained for ammonium sulfate (circles) and sodium chloride (squares) are in good agreement. The data show little scatter ($R^2=0.99$), making the calibration quite precise. The uncertainties of S_{exp} are found to be below 0.06% (absolute) for all sizes and compositions, comparable to the variations due to temperature fluctuations. The overall uncertainty (one standard deviation) of the supersaturation setting of the instrument is estimated to be ±(0.05+0.05·S)%, where the first term is connected to the temperature fluctuations of the plates, and the second term to the uncertainty of the calibration. A second calibration, performed a year later, yielded slightly different regression constants, caused by changes made to the chamber, but was similarly precise.

3.3 Number concentration calibration

The CCN counter was calibrated with respect to number concentration, by selecting particle diameters so that the critical supersaturation for activation was well below the supersaturation set in the instrument. Thus, all particles entering the CCN chamber were activated, including multiply charged particles of larger size. Calibration curves can be derived by relating the CCN concentrations to the number of particles entering the CCN counter (CN), which were counted in the CPC.

In the first calibration experiment we focused on the instrument's behavior at rather high number concentrations, while the second set of measurements explored the effect of different supersaturations on the observed CCN number concentrations. Figure 4 shows the calibration results of the first experiment. Although we were aware that problems due to water vapor depletion might be important at concentrations above $1000\,cm^{-3}$, we extended the calibration up to $25\,000\,cm^{-3}$ to explore if data at higher concentrations could still be used.

At low concentrations, a good 1:1 agreement can be observed, assuming a measuring volume of $0.075\,cm^3$, which had been determined in previous calibrations. Coincidences, i.e. when two droplets are counted as one due to overlap in the picture, appear at concentrations above $\sim 1700\,cm^{-3}$. The image analysis software uses an empirical correction for coincidence effects, which does not seem to perform adequately at very high droplet concentrations. A calibration function can still be derived from Fig. 4a, however, at high concentrations it cannot be strictly applied to particles with a composition other than the calibration salt, ammonium sulfate. Particles with a different chemical composition can have a different growth behavior, thus changing the effects of coincidence. For example, using the calibration from Fig. 4a in a study of biomass burning smoke particles (which don't grow as large as ammonium sulfate particles at the same S) leads to overcompensation for the coincidence effect at high concentrations, resulting in CCN concentrations higher than the aerosol particle concentration. We concluded that, when measuring particles of other composition than the calibration

ACPD
6, 2151–2174, 2006

EGU

particles, the coincidence effects make it impossible to obtain reliable data at concentrations above ~5000 cm^{-3}.

Figure 4b shows that CCN concentrations below ~300 cm^{-3} are slightly overestimated. The reason for this is probably that at low concentrations the statistical fluctuations in droplet number are relatively larger, and since the calculation of the CCN concentration is based on the image with the highest number of droplets, this leads to an overestimation of the concentration (Dusek et al., 2006).

At low concentrations a relatively large spread in the measured CCN concentration can be observed, which induces a large uncertainty in the calibration. Due to the small sensing volume (0.075 cm^3), a CCN concentration of approximately 40 cm^{-3} corresponds to three droplets in an image. One standard deviation of the measured CCN concentration (σ_{CCN}) can be estimated (assuming Poisson distribution of the number of droplets in the measuring volume) as:

$$\sigma_{CCN} = \sqrt{\frac{CCN}{V}} \quad (2)$$

This estimation agrees well with the observed variation, but is only valid in the range where the coincidence effects are low (<~5000). The lower detection limit is concluded to be around a concentration of 100 CCN cm^{-3}, with a relative uncertainty of ±37% (1σ).

In the second calibration experiment, we studied the dependence of counting efficiency on supersaturation. The use of the photographic technique has previously often been assumed to show no dependence of the counting efficiency on supersaturation. Therefore the calibration of the sensing volume is commonly performed only at high S (e.g. Giebl et al., 2002; Dusek et al., 2006) and the picture(s) with the highest count is used to calculate the CCN concentration. However, we found a dependence of the CCN/CN ratio on the supersaturation (Fig. 5). The reason for this dependence seems mainly to be caused by different growth behavior at different S. Figure 6 shows an example from a calibration using monodisperse ammonium sulfate particles. The growth at lower S is delayed and more spread out with time. This results in a lowering of the

ACPD
6, 2151–2174, 2006

EGU

maximum count at lower S. Other reasons might be a decrease of the intensity of the laser beam at the edges of the sensing volume, or inhomogeneous illumination at the edges of the laser beam due to diffraction patterns caused by the slit in front of the laser. In these regions, large particles (at high S) would be bright enough to be visible, whereas small particles (at low S) could be so dim that they are not counted. However, while this was not investigated in detail, we can still conclude that even for instruments using the photographic technique, it is important to make number calibrations as a function of supersaturation. The use of a sensing volume derived from calibrations at high S could lead to a considerable underestimate of the CCN concentrations at low supersaturations.

3.4 Study of the water vapor depletion

During droplet growth, water vapor is depleted, and if the diffusion is not fast enough to maintain the equilibrium, the supersaturation in the chamber will decrease. This effect has been theoretically evaluated by several authors. Squires (1972) and Nenes et al. (2001) state that for CCN concentrations up to 1000 cm^{-3} the effect is negligible, whereas Ji et al. (1998) state that the effect can already be important for concentrations higher than 100 cm^{-3}, and Holländer et al. (2002) state that it can already be of importance at concentrations of 10 cm^{-3}. We made measurements using ammonium sulfate particles of 37 nm in diameter, and varied the CCN number concentration between 32 and 4000 cm^{-3}. The calculated critical supersaturation for activation for this size is 0.72%. The experimentally obtained values, as a function of concentration, can be found in Table 1. We observe no evidence for the proposed lowering of the supersaturation. The observed variation is within the uncertainty of the supersaturation.

ACPD
6, 2151–2174, 2006

4 Conclusions

A static (parallel-plate thermal-gradient) diffusion chamber (SDC) CCN counter that uses a video camera and image processing methods to count the number of activated CCN, was characterized. The results obtained gives a larger understanding why and in which way it is necessary to calibrate the SDC CCN counter. We found that, because of difficulties to precisely measure the temperatures at the plates, it is essential to experimentally calibrate SDC CCN counters with respect to supersaturation, and not base the supersaturation only on the theoretical description of the instrument and the temperatures measured inside the plates. For SDC CCN counters using detection of light scattering as a measure of the CCN concentration, the number calibration has to be performed as a function of supersaturation, since the amount of scattered light also depends on the size of the droplets, and the growth rate is proportional to the supersaturation. The use of a video or CCD camera and image analyses software should ideally avoid this dependence, since individual droplets are counted. However, we found a dependence on supersaturation, probably mainly because of different droplet growth behavior at different supersaturations. It is therefore important to perform the number calibration as a function of supersaturation also for this type of CCN counter. We did not investigate the dependence of CCN number concentration on particle type and particle size, since Delene and Deshler (2000) found that this effect is minor (within the uncertainty of the instrument). However, we found that the highest detectable concentration is limited by coincidence effects, and that these effects are difficult to quantify when measuring particles of other chemical composition than the calibration particles. Finally, we studied the proposed effect of a reduction of the supersaturation because of water vapor depletion at high CCN concentrations. To our knowledge, this effect has previously only been theoretically investigated. We observed no evidence for the proposed effect, in the range up to 4000 CCN cm^{-3}.

ACPD
6, 2151–2174, 2006

EGU

Appendix A

Determination of theoretical supersaturation in the SDC CCN counter

For convenience we derive here the theoretical supersaturation profile of the SDC CCN chamber. This derivation is relatively simple to do but not readily available in the literature. The static thermal-gradient CCN counter works with a temperature difference between two horizontal wetted plates, the lower plate colder than the upper to eliminate buoyant convection in the chamber. In equilibrium this gives rise to linear gradients of temperature and water vapor partial pressure between the two plates. Because of the non-linear dependence of the saturation vapor pressure on temperature, a parabolic supersaturation profile will be established.

Relative humidity (RH) can be calculated as the ratio between the partial pressure of water vapor (e_w) to the saturation vapor pressure at the same temperature ($e_{\mathrm{sat},w}$), and the supersaturation (S) is related to RH as:

$$RH = \frac{e_w}{e_{\mathrm{sat},w}} \cdot 100\% \qquad S = RH - 100\% \tag{A1}$$

Since the water vapor is assumed to be in equilibrium at the wetted surfaces of the plates, the partial water vapor pressures just next to the plates are the same as the saturation vapor pressures at the temperatures of the surfaces of the lower and upper plates respectively, T_l and T_u. The saturation vapor pressure over a flat water-surface can for example be calculated using the approximate formula given in the Appendix of Pruppacher and Klett (1997). It is also assumed that water vapor can be considered as an ideal gas, which is a reasonable assumption (Pruppacher and Klett, 1997). Due to the difference in temperatures and partial pressures of water vapor between the plates, it is assumed that heat and molecular diffusion will establish a linear gradient of temperature (T) and water vapor partial pressure (e_w) in the chamber:

$$T(z) = \frac{T_u - T_l}{H} \cdot z + T_l \qquad e_w(z) = \frac{e_{\mathrm{sat},w}(T_u) - e_{\mathrm{sat},w}(T_l)}{H} \cdot z + e_{\mathrm{sat},w}(T_l) \tag{A2}$$

ACPD
6, 2151–2174, 2006

EGU

where H is the distance between the plates and z is the height (Katz and Mirabel, 1975). In equilibrium, the supersaturation profile in the chamber can thus be calculated by:

$$S(z) = \left(\frac{e_w(z)}{e_{\mathrm{sat},w}(T(z))} - 1 \right) \cdot 100\% \tag{A3}$$

An example with temperatures of 25 and 20°C is presented in Fig. A1. The maximum supersaturation will be reached close to the center of the chamber and can be approximated as:

$$S\left(H/2\right) = \left(\frac{\frac{e_{\mathrm{sat},w}(T_l)+e_{\mathrm{sat},w}(T_u)}{2}}{e_{\mathrm{sat},w}\left(\frac{T_l+T_u}{2}\right)} - 1 \right) \cdot 100\% \tag{A4}$$

Acknowledgements. We thank M. Bilde and B. Svenningsson, University of Copenhagen, Denmark, for help with the calibrations. This work was funded by the Max Planck Society, Germany.

References

Bilde, M. and Svenningsson, B.: CCN activation of slightly soluble organics: the importance of small amounts of inorganic salts and particle phase, Tellus, 56B, 128–134, 2004.

Corrigan, C. E. and Novakov, T.: Cloud condensation nucleus activity of organic compounds: a laboratory study, Atmos. Environ., 33, 2661–2668, 1999.

Cruz, C. N. and Pandis, S. N.: A study of the ability of pure secondary organic aerosol to act as cloud condensation nuclei, Atmos. Environ., 31, 2205–2214, 1997.

Delene, D. J., Deshler, T., Wechsler, P., and Vali, G. A.: A balloon-borne cloud condensation nuclei counter, J. Geophys. Res., 103(D8), 8927–8934, 1998.

Delene, D. J. and Deshler, T.: Calibration of a photometric cloud condensation nucleus counter designed for deployment on a balloon package, J. Atmos. Ocean. Tech., 17, 459–467, 2000

Dusek, U., Reischl, G., and Hitzenberger, R.: CCN activation of pure and coated black carbon particles, Environ. Sci. Technol., 40(4), 1223–1230, doi:10.1021/es0503478, 2006.

Giebl, H., Berner, A., Reischl., G., Puxbaum, H., Kasper-Giebl, A., and Hitzenberger, R.: CCN activation of oxalic and malonic acid test aerosols with the University of Vienna cloud condensation nuclei counter, J. Aerosol Sci., 33, 1623–1634, 2002.

Hinds, W. C.: Aerosol Technology – properties, behaviour and measurements of airborne particles, 2nd ed., John Wiley & Sons, Inc., 1999.

Holländer, W., Dunkhorst, W., Lödding, H., and Windt, H.: Theoretical simulation and experimental characterization of an expansion-type Kelvin spectrometer with intrinsic calibration, J. Atmos. Ocean. Techn., 19, 1811–1825, 2002.

Hudson, J. G.: Cloud Condensation Nuclei, J. Appl. Meteorol., 32, 596–607, 1993.

Jennings, S. G., Geever, M., and O'Connor, T. C.: Coastal CCN measurements at Mace Head with enhanced concentrations in strong winds, Atmos. Res., 46, 243–252, 1998.

Ji, Q., Shaw, G. E., and Cantrell, W.: A new instrument for measuring cloud condensation nuclei: Cloud condensation nucleus "remover", J. Geophys. Res., 103(D21), 28 013–28 019, 1998.

Jokinen, V. and Mäkelä, J. M.: Closed-loop arrangement with critical orifice for DMA sheath/excess flow system, J. Aerosol Sci., 28(4), 643–648, 1997.

Katz, J. L. and Mirabel, P.: Calculation of supersaturation profiles in thermal diffusion cloud chambers, J. Atmos. Sci., 32, 646–652, 1975.

Lala, G. G. and Jiusto, J. E.: An automatic light scattering CCN counter, J. Appl. Meteorol., 16, 413–418, 1977.

Low, D. H.: A theoretical study of nineteen condensation nuclei, Journal de Recherches Atmosphériques, 4, 65–78, 1969.

Mitra, S. K., Brinkmann, J., and Pruppacher, H. R.: A wind tunnel study on the drop-to-particle conversion, J. Aerosol Sci., 23, 245–256, 1992.

McMurry, P. H.: A review of atmospheric aerosol measurements, Atmos. Environ., 34, 1959–1999, 2000.

Nenes, A., Chuang, P. Y., Flagan, R. C., and Seinfeld, J. H.: A theoretical analysis of cloud condensation nucleus (CCN) instruments, J. Geophys. Res., 106(D4), 3449–3474, 2001.

de Oliveira, J. C. P. and Vali, G.: Calibration of a photoelectric cloud condensation nucelus counter, Atmos. Res., 38, 237–248, 1995.

Otto, P., Georgii, H.-W., and Bingemer, H.: A new three-stage continuous flow CCN-counter, Atmos. Res., 61, 299–310, 2002.

Pruppacher, H. R. and Klett, J. D.: Microphysics of Clouds and Precipitation, 2. ed. Kluwer

Academic Publishers, Dordrecht, The Netherlands, 1997.
Roberts, G. C., Andreae, M. O., Zhou, J., and Artaxo, P.: Cloud condensation nuclei in the Amazon Basin: "Marine" conditions over a continent?, Geophys. Res. Lett., 28(14), 2807–2810, 2001.
Roberts, G. C.: Cloud condensation nuclei in the Amazon Basin: their role in a tropical rainforest, PhD thesis, 2001.
Roberts, G. C., Nenes, A., Seinfeld, J. H., and Andreae, M. O.: Impact of biomass burning on cloud properties in the Amazon Basin, J. Geophys. Res., 108(D2), 4062, doi:10.1029/2001JD000985, 2003.
Roberts, G. C. and Nenes, A.: A continuous-flow streamwise thermal-gradient CCN chamber for atmospheric measurements, Aerosol Sci. Technol., 39, 206–221, 2005.
Snider, J. R. and Brenguier, J.-L.: Cloud condensation nuclei and cloud droplet measurements during ACE-2, Tellus 52B, 828–842, 2000.
Snider, J. R., Guibert, S., Brenguier, J.-L., and Putaud, J.-P.: Aerosol activation in marine stratocumulus clouds: 2. Köhler and parcel theory closure studies, J. Geophys. Res., 108(D15), 8629, doi:10.1029/2002JD002692, 2003.
Squires, P.: Diffusion chambers for the measurement of cloud nuclei, Journal de Recherches Atmosphériques, 6, 565–572, 1972.
Twomey, S.: The nuclei of natural cloud formation Part I: The chemical diffusion method and its application to atmospheric nuclei, Geofisica pura e applicata, 43, 227–242, 1959.
VanReken, T. M., Nenes, A., Flagan, R. C., and Seinfeld, J. H.: Concept for a new cloud condensation nucleus (CCN) spectrometer, Aerosol Sci. Technol., 38, 639–654, 2004.
Wieland, W.: Die Wasserdampfkondensation an natürlichem Aerosol bei geringen Übersättigungen, Zeitschrift für Angewandte Mathematik und Physik, 7, 428–460, 1956.
Young, K. C. and Warren, A. J.: A reexamination of the derivation of the equilibrium supersaturation curve for soluble particles, J. Atmos. Sci., 49, 1138–1143, 1992.

Table 1. Observed critical supersaturation for activation as a function of CCN concentration.

CCN concentration cm^{-3}	Supersaturation %
32	0.71
100	0.74
450	0.73
1000	0.69
1800	0.71
2200	0.73
4000	0.74

ACPD
6, 2151–2174, 2006

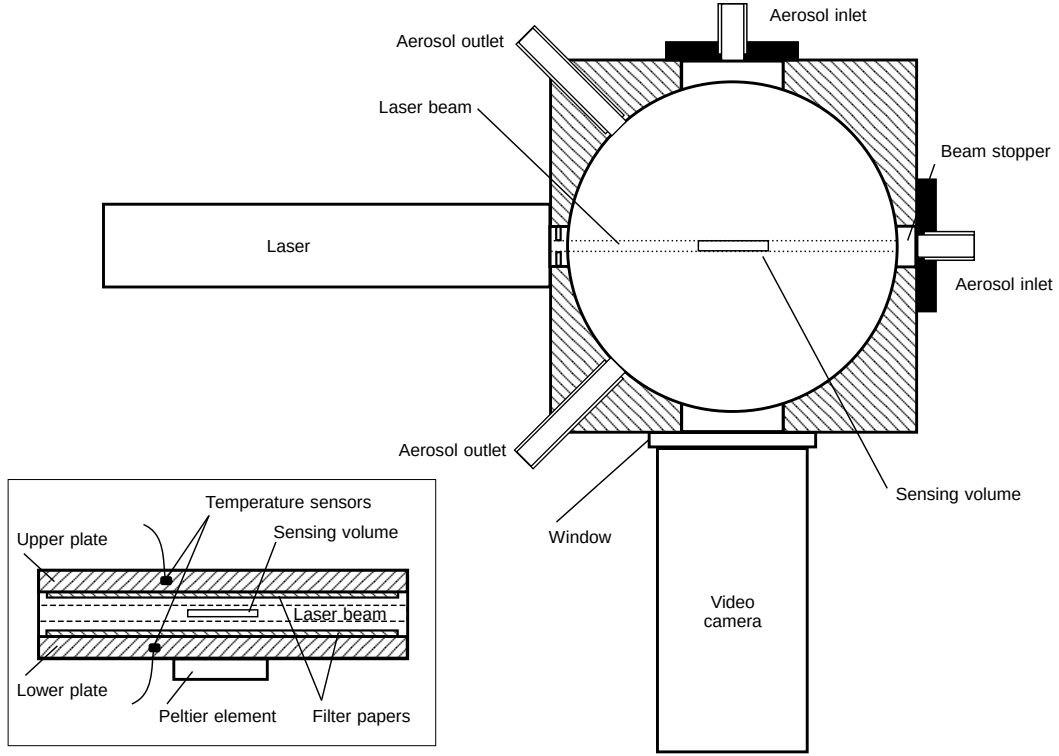

Fig. 1. Schematic of the chamber of the Mainz CCN counter, seen from above. Insert: View of the chamber as seen from the side.

ACPD
6, 2151–2174, 2006

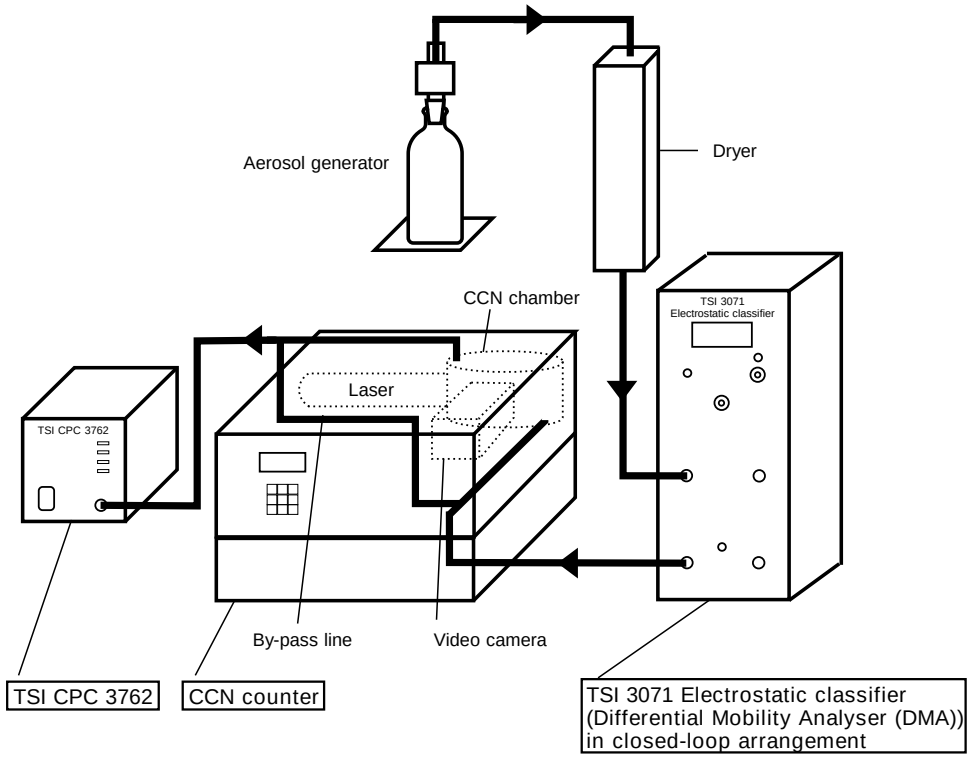

Fig. 2. The calibration set-up, consisting of a DMA, the CCN counter and a CPC (the CPC is not needed for the supersaturation calibration).

ACPD
6, 2151–2174, 2006

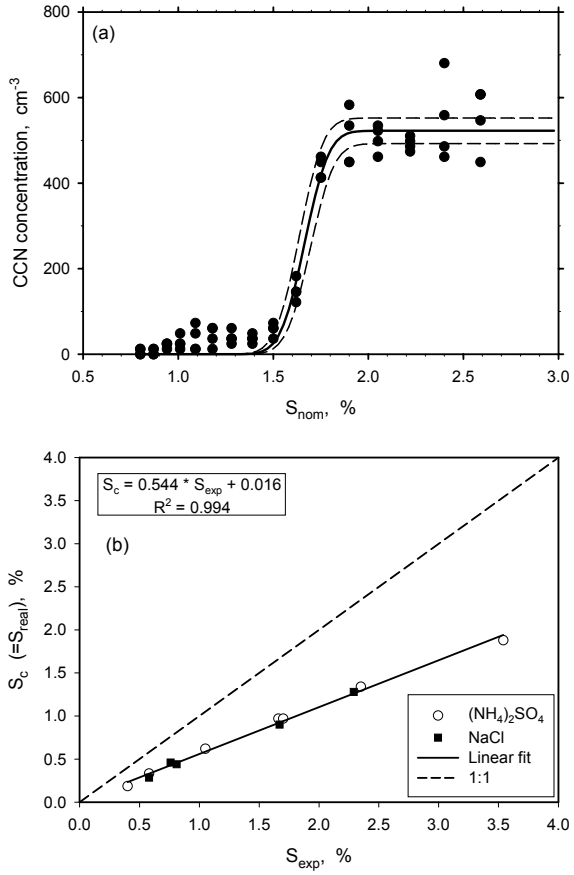

Fig. 3. **(a)** Activation spectrum of 30 nm ammonium sulfate particles. The solid line is the fitted function, and the dashed lines are the upper and lower bounds, calculated from the 95% confidence intervals of the fitted variables. **(b)** Results from the supersaturation calibration, nominal (S_{exp}) versus actual (S_c) supersaturation in the CCN counter. The function is the linear regression fit.

ACPD
6, 2151–2174, 2006

EGU

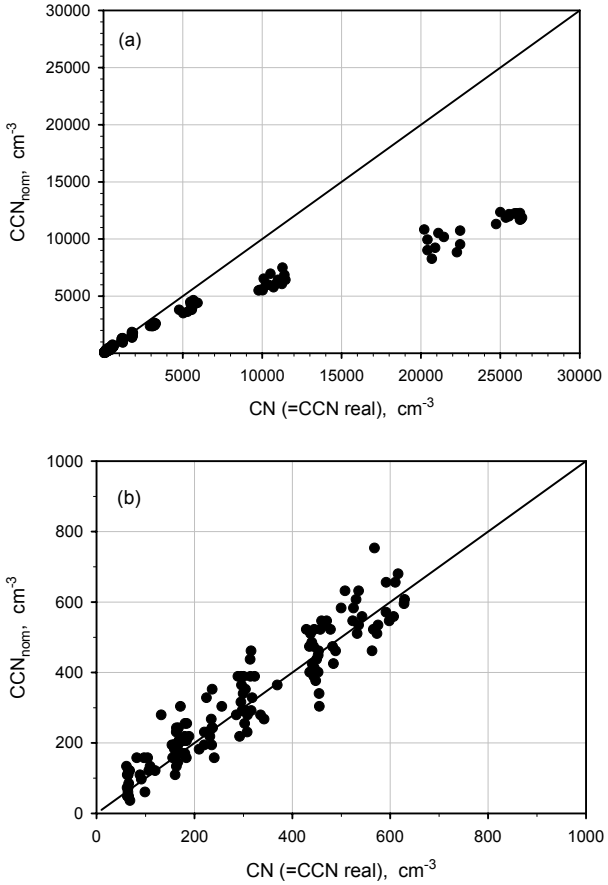

Fig. 4. Number calibration. **(a)** Scale: 0–30 000 cm^{-3}, **(b)** Scale: 0–1000 cm^{-3}.

ACPD
6, 2151–2174, 2006

EGU

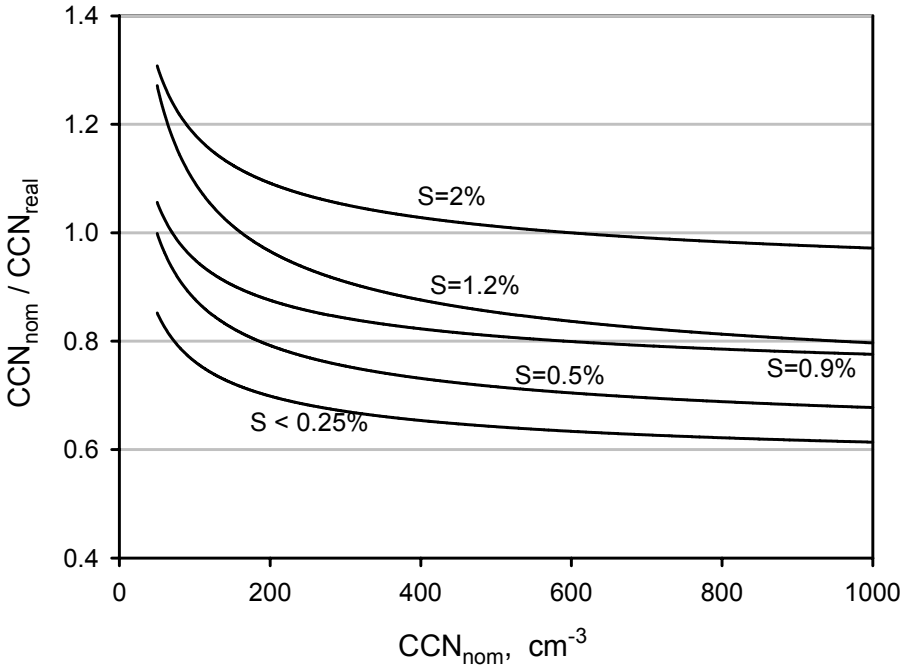

Fig. 5. Dependence of measured CCN concentration (CCN_{nom}) on supersaturation (S), fitted curves.

ACPD
6, 2151–2174, 2006

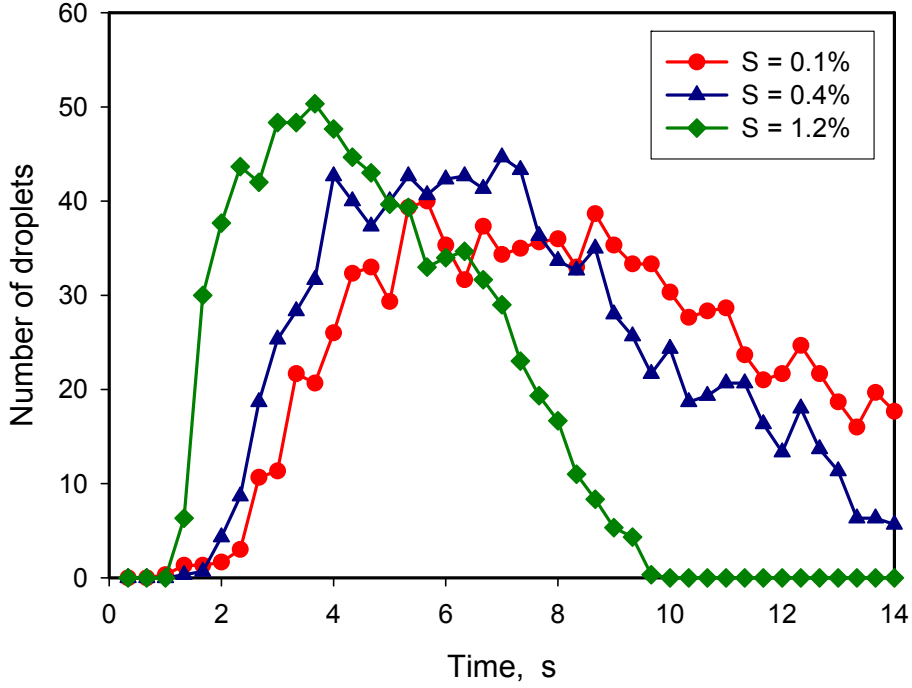

Fig. 6. Number of droplets counted per image, showing the droplet growth in the chamber as a function of time, at three different supersaturations. The results were obtained at a calibration with monodisperse ammonium sulfate particles of 250 nm in diameter. Three images per second were taken.

ACPD
6, 2151–2174, 2006

EGU

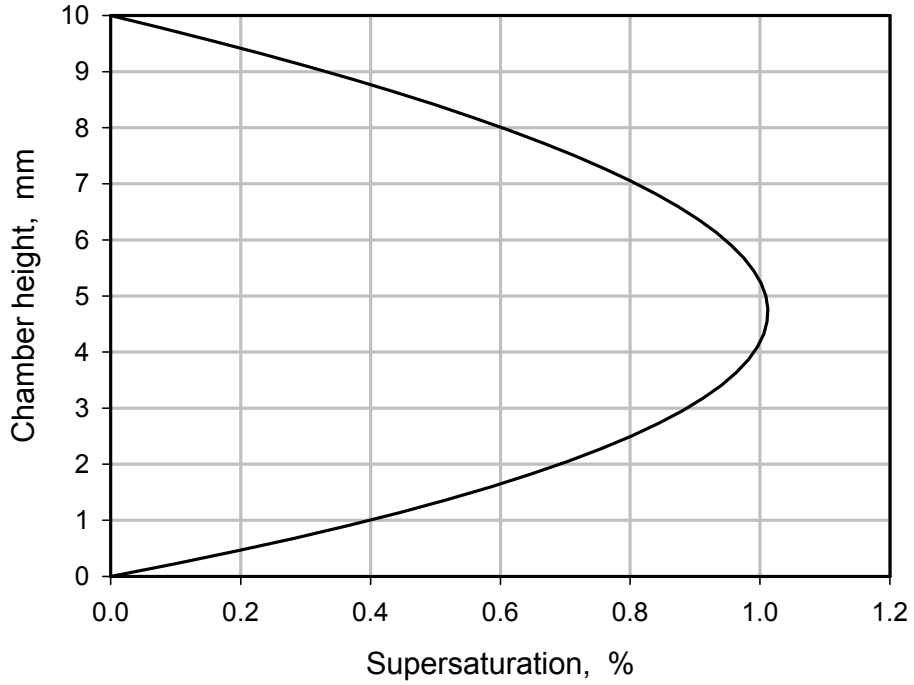

A1. Supersaturation profile in the CCN chamber, with upper plate temperature of 25°C, lower plate temperature of 20°C, and a chamber height of 10 mm.